Multimed Tools Appl
DOI 10.1007/s11042-017-4973-6

Single image fog and haze removal based on self-adaptive guided image filter and color channel information of sky region

Bo Jiang[1] · **Hongqi Meng**[1] · **Jian Zhao**[1] · **Xiaolei Ma**[2] · **Siyu Jiang**[3] · **Lin Wang**[1] · **Yan Zhou**[1] · **Yi Ru**[1] · **Chao Ru**[1]

Received: 22 October 2016 / Revised: 15 April 2017 / Accepted: 21 June 2017

Abstract In this paper, we report an effective algorithm for removing both fog and haze from a single image. Existing algorithms based on atmospheric degeneration model generally lead to non-definite solutions for the haze and thick fog images, though they are very efficient for thin fog images. In general, as the algorithms based on vision enhancement cannot automatically adjust weight coefficient for the different structure images, the excessive or inadequate enhancement may emerge. In this paper an original degradation image is primarily segmented into the sky and non-sky regions, and then the main boundaries of non-sky region are extracted using L_0 smoothing filter. So our vision enhancement algorithm automatically adjusts weight coefficient according to various structure images. At the stage of vision enhancement, guided image filter famous for its excellent boundary preservation is adopted. As for haze image, the color channel information scattered by haze particles can be obtained in the sky region to make an effective color correction. Both the subjective and objective evaluations of experimental results demonstrate that the proposed algorithm has more outstanding recovery effect for haze and thick fog images. Moreover, the proposed algorithm can judge fog or haze image, which is a by-product of this research.

Keywords Fog and haze removal · Color correction · Main boundaries extraction

✉ Bo Jiang
jiangbo@nwu.edu.cn

[1] School of Information and Technology, Northwest University, Xi'an 710127, People's Republic of China

[2] Department of Physics, Emory University, Atlanta, Georgia 30322, USA

[3] School of Electronic and Information Engineering, Xi'an Jiaotong University, Xi'an 710049, People's Republic of China

Published online: 20 July 2017

1 Introduction

As the air quality continues to deteriorate, the emergence frequency of fog/haze weather has obviously increased. Under fog/haze weather conditions, the image degradation is primarily caused by the scattering of fog/haze particles [16], and the scattering intensity of these particles is enhanced along with the distance increases between the scene and imaging device. More specifically, the aforementioned phenomenon can be basically explained by two reasons: (1) The light intensity of scene is attenuated in the process of light transmitting from the scene to imaging device with the transmission distance increases. (2) In the fog/haze weather, the scattering light of non-scene may enter the imaging device and participates in imaging due to the existence of fog/haze particles in the atmosphere. The combination of aforementioned reasons gives rise to the image degeneration in the aspect of contrast and saturation, which is disadvantageous to higher level image analysis and processing [3, 7, 13, 15]. The aforementioned imaging principle under fog/haze weather conditions is schematically shown in Fig. 1.

The research on fog removal has hitherto made considerable progress, and the algorithms can be grouped into two types. One is based on the vision enhancement and the other adopts atmospheric degradation model [3, 8]. For the former, the corresponding algorithms aim at a global or local atmospheric correction for fog image in order to visually recover the original fog-free image to the greatest extent. This type of algorithms has the advantages of low computational complexity and extensive applications. For the latter, it focuses on the mechanism of image degradation, and the fog layer can be removed by establishing the atmospheric degradation model, which can be further solved by the various prior constraints. Due to considering the deep-level mechanism of image degradation, the information loss in the process of imaging under fog weather conditions can be accurately compensated, as a result, the latter type of algorithms has rapidly become the main trend in the field of image fog removal.

However, the existing algorithms for fog removal do not fit for image haze removal, which is primarily due to different scattering properties between fog particle and haze particle. The average diameter of fog particles is generally larger than the visible-light wavelength, so the scattering intensity is approximately equal for different wavelength visible-light. As a result, the overall color of fog layer is close to milky white or green white. By contrast, the average diameter of haze particles is normally smaller than the visible-light wavelength. In this case,

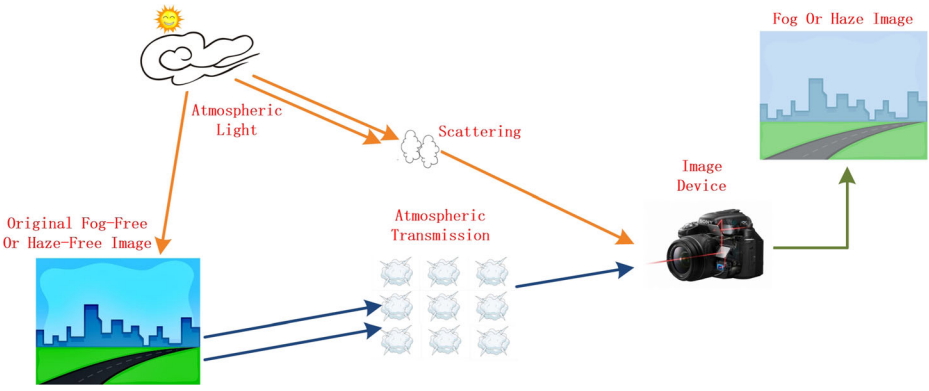

Fig. 1 The diagrammatic sketch of imaging principle under fog/haze weather conditions

the scattering intensity of haze particles depends on the wavelength of visible-light itself, and it can lead to the short-wavelength components scattered enormously. Moreover, the distribution of haze has longer vertical distance than that of fog. Therefore, for the distant sky region, the short-wavelength components in the visible-light, i.e., cyan, blue and purple light, are almost completely scattered away before reaching the imaging device. For the same reason, if there are numerous haze particles in the atmosphere, the short-wavelength components are also completely scattered away. In these cases, the imaging color is close to the mixture of long-wavelength visible-light, i.e., the mixture of red, orange and yellow lights.

Due to the different scattering properties between the fog and haze particles, the algorithms based on atmospheric degradation model may fail to achieve haze removal though they work excellently for fog removal. The reason is that the scattering coefficients are no longer consistent for different wavelength visible-light, and the aforementioned consistent is widely used to solve the atmospheric degradation model. More specifically, the thick fog layer also makes the scattering coefficient inconsistent because the above approximate condition for thin fog is no longer right for thick fog with strong scattering. As a result, it can lead to non-definite solutions to atmospheric degradation model for haze and thick fog images.

As for the traditional vision enhancement algorithms, they are prone to cause the phenomenon of excessive or inadequate enhancement, which makes the application of this type of algorithms limited. Considering the particularity of imaging in the haze and thick fog conditions, we focus on the vision enhancement type by the theory of guided image filtering, which is famous for its excellent performance of boundary preservation. This theory is proposed by He [4]. It should be pointed out that the image boundaries cannot be completely preserved since the solution to the model of guided image filter is an approximate solution in practice.

In this paper, an original degradation image is segmented into the sky and non-sky regions as pre-treatment by our previous work [5]. Combined with the L_0 smoothing filter, the main boundaries in the non-sky region can be extracted and the crucial weight coefficient in the process of guided image filtering enhancement can be reasonably determined in a self-adaptive fashion, and it can avoid the phenomenon of excessive or inadequate enhancement. Furthermore, the color channel information of sky region is used to make a further color correction for haze image. The proposed algorithm is experimentally demonstrated to work effectively for both the haze image and thick fog image from both the subjective and objective evaluations. In addition, the fog and haze images can be classified by the proposed algorithm, which is a by-product of this work.

The framework of this paper is organized as follows. Section 2 discusses the existing algorithms targeting image fog removal rather than haze removal. In Section 3 the proposed algorithm is introduced, and the experimental results are shown in Section 4 to demonstrate the effectiveness of the proposed algorithm. The paper is ultimately concluded in Section 5.

2 Related work

As introduced in Section 1, the research on image fog removal has already gained huge advances, and numerous corresponding algorithms have been proposed. Typically, the mean filter is taken by Tarel [10] to estimate the atmospheric degradation model, and the recovery image is subsequently obtained using the tone mapping. The most prominent feature of this algorithm is the fast processing speed and effective recovery effect for fog image. Based on the

atmospheric degradation model, Fattal [1] assumes that the reflection intensity of local region in a fog image is constant, and the independent component analysis is adopted to estimate the scene reflection intensity. It should be addressed that these classical algorithms are effective under thin fog weather conditions.

Shortly afterwards, an eminent algorithm for image fog removal is proposed by He [3], and the improved algorithms have subsequently emerged [2, 6, 11, 14]. In the algorithm of He, based on the statistics of numerous natural fog-free images, dark channel prior is proposed to obtain the atmospheric light value and transmission map, and then the atmospheric degradation model can be solved to estimate the original fog-free image. Subsequently, a new guided image filter is proposed also by He [4], and it is used to optimize the process of estimating transmission map to improve the calculating accuracy and speed. Note that guided image filter is staying at the stage of optimizing transmission map here, and the proposed algorithm uses this filter at the stage of image fog/haze removal directly. By the algorithm of He [3], the excellent results are obtained, but it is only fit for thin fog image. Under haze and thick fog conditions, this algorithm fails to solve atmospheric degradation model. This paper aims at solving the problems above in the related work.

3 Algorithm in this paper

This section describes the proposed algorithm, which can not only work effectively for thick fog image but also for haze image. The difference between the thick fog removal and haze removal is reflected in the step of color correction in the proposed algorithm. In order to completely describe the recovery process of proposed algorithm, the recovery process of haze removal is introduced as an example. Based on the analysis above, the existing algorithms have two limitations that haze image and thick fog image cannot be effectively processed. Motivated by this challenge, a fog/haze removal algorithm based on self-adaptive guided image filtering is proposed in this paper. The original fog/haze image is segmented into the sky and non-sky regions firstly, and then the main boundaries of non-sky region are extracted using L_0 smoothing filter [12], so the crucial weight coefficient of enhancement can be automatically adjusted according to the main boundaries above. The vision enhancement based on the guided image filtering in a self-adaptive coefficient fashion can be realized eventually. Moreover, the proposed algorithm can be used to judge fog or haze image. The schematic diagram of proposed algorithm is shown in Fig. 2.

Fig. 2 The schematic diagram of proposed algorithm

3.1 Self-adaptive weight coefficient

The sensitivity of human eyes to various structural information in an image is different. According to the physiological property of human visual system, the main boundaries in an image are the most sensitive information, which is the foundation for human eyes to recognize scene object and estimate scene distance. The more complex the scene structure is, the larger the number of boundary pixels will be. Due to the excessive enhancement caused by enhancement recovery often appears for the image with complex structure, a smaller weight coefficient for enhancement recovery should be adopted in this conditions. On the contrary, for the image with simple structure, a larger weight coefficient is preferred.

In general the sky region contains little boundary information, so the non-sky region is extracted and used to calculate the weight coefficient. It not only facilitates determining the crucial coefficient based on actual scenes but also facilitates further reducing the algorithm complexity. In general, the image segmentation algorithms strongly depend on the image boundary, which makes it difficult to perform for fog/haze images with degraded boundary information. For this reason, an effective algorithm for non-sky region segmentation under fog/haze weather conditions is adopted, which is proposed in our previous work [5]. With this algorithm, the non-sky region can be easily and quickly extracted without any pre-processing. Note that the test images in this paper are mainly taken from the Internet.

However, the statistics of image boundaries directly from non-sky region may contain the irrelevant tiny structures, e.g. the doors and windows of one building, which makes it disadvantageous to determine the self-adaptive weight coefficient reasonably. In order to effectively extract the main boundaries in non-sky region, the L_0 smoothing filtering [12] is taken as the pre-processing operation in this paper. To an input image S, assuming that the gradient of any pixel j in its filtered image $\tilde{S}$ can be expressed as $\nabla\tilde{S}_j = \left(\partial_x\tilde{S}_j, \partial_y\tilde{S}_j\right)$, where ∂_x and ∂_y are the gradients of pixel j at horizontal direction of x and vertical direction of y respectively. Then the statistics of non-zero gradient pixels in the filtered image $\tilde{S}$ can be expressed by:

$$C\left(\tilde{S}\right) = \#\left\{j \middle| \left|\partial_x\tilde{S}_j\right| + \left|\partial_y\tilde{S}_j\right| \neq 0\right\} \tag{1}$$

where $C\left(\tilde{S}\right)$ is defined as a counter to count the number of the pixels with non-zero gradient, and $\tilde{S}$ can be estimated by:

$$\min_{\tilde{s}} \left\{ \sum_j \left(\tilde{S}_j - S_j\right)^2 + \lambda \cdot C\left(\tilde{S}\right) \right\} \tag{2}$$

where $\sum_j \left(\tilde{S}_j - S_j\right)^2$ is the data fidelity term, which is used to ensure the maximum similarity between the input image S and filtered image $\tilde{S}$. λ is the filter coefficient, and the higher the value λ is, the more smoothing the filtered image $\tilde{S}$ will be.

The aforementioned filtering is called L_0 smoothing filtering, and it can be used as the pre-processing of extracting main boundary information. With such a filter, the main boundaries in the non-sky region can be effectively preserved and further extracted, meanwhile, the detail structure information is filtered away. By doing this, the real complexity of scene structure can be used to determine the weight coefficient in a self-adaptive fashion. Fig. 3a shows the original haze image, and Fig. 3b and c show the extracted non-sky region before and after L_0

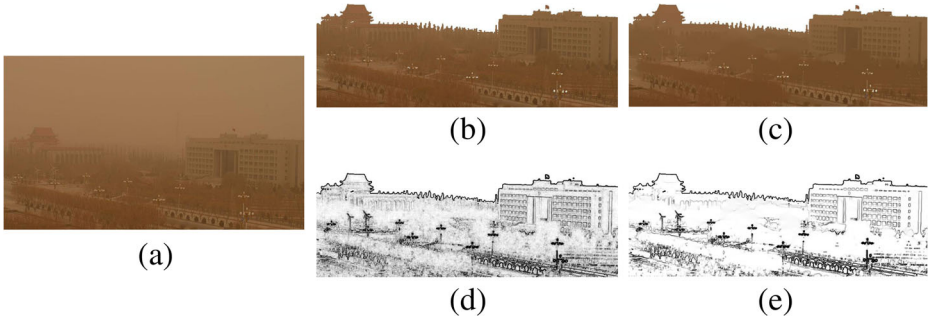

Fig. 3 Extracting the main boundaries of non-sky region: (**a**) Original haze image, (**b**) Non-sky region before L_0 smoothing filtering, (**c**) Non-sky region after L_0 smoothing filtering, (**d**) Boundaries of (**b**), (**e**) Boundaries of (**c**)

smoothing filtering respectively, and binarization boundary images of Fig. 3b and c are illustrated in Fig. 3d and e respectively. Note that the color reversal is adapted to the images of binarization boundary here in order to facilitate observation. One can easily see that the boundaries after L_0 smoothing filtering is more advantageous to accurately extract the main boundaries of non-sky region.

In the non-sky region, we define h as the important ratio between the pixel number of main boundaries and that of entire region. Here the main boundaries of non-sky region are extracted based on the image after L_0 smoothing filtering. Then the crucial self-adaptive weight coefficient τ can be defined as:

$$\tau = N(1-h), \quad \tau \in [2, 7] \tag{3}$$

where N is a constant for obtaining the more reasonable τ value. Basically, for a haze image, the N value is set to 4 or 5 and is slightly higher for a fog image. In addition, the intensity of enhanced image is linearly related to the self-adaptive weight coefficient τ in Eq. (3). Avoid acquiring τ with too high or too low value for some special images, its value is limited in [2, 7]. Furthermore, in order to calculate the weight coefficient in a self-adaptive fashion, N value is fixed to 4 for the haze image while is fixed to 7 for the fog image in this paper.

Fig.4 shows the values of self-adaptive weight coefficient τ calculated according to the original images with the complexity decreasing in turn. As can be seen, with the image complexity decreasing, the value of self-adaptive weight coefficient increases to meet the need of image enhancement.

3.2 Image haze removal based on self-adaptive guided image filtering

Differently from the imaging principle under thin fog weather conditions, the light intensity after scattering by the haze particles mainly depends on the visible-light wavelength, which leads to the uncertainty of atmospheric scattering coefficient, and this problem cannot be effectively solve by the mainstream algorithms based on atmospheric degradation model. Note that the thick fog conditions can also bring the problem above. This paper applies the guided image filter [4] to the research of image haze removal, and takes the particularity mechanism of light scattering by the haze particles into account. Guided image filter is developed on the basis of bilateral filter, and it is an excellent boundary preserving filter. Assuming that the original image is expressed by p, and the image after guided filtering expressed by q is linearly related

N =4: τ=2.000 (a)

N =4: τ=3.5583 (b)

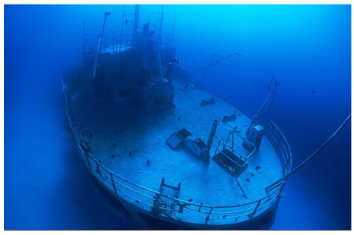

N =7: τ=5.6934 (c)

N =7: τ=6.3255 (d)

Fig. 4 Self-adaptive weight coefficients calculated according to original images with different complexity

to the guide image D in a local template ω_k centered at the pixel k.The filtered image q in this template can be written as:

$$q_i = a_k D_i + b_k, \forall i \in \omega_k \tag{4}$$

where (a_k, b_k) is the constant coefficients in the template ω_k, and the pixel i is involved in all overlapping templates that cover i collectively. Taking the gradient operation for both sides of Eq. (4), we can get $\nabla q_i = a_k \nabla D_i$, which means that the filtered image and guide image have the same boundaries in theory. Based on the definition above, the filtered image q can be obtained and the difference $(p-q)$ is regarded as the image boundaries. Here the image noise is neglected temporarily. Ultimately, the image boundaries is amplified by τ times and then added to q, so the haze removal result based on image enhancement can be expressed as:

$$I_e = q + \tau\,(p-q) \tag{5}$$

where τ is the crucial self-adaptive weight coefficient stated in Section 3.1. Through this simple Eq. (5), we can obtain the effective recovery result with low algorithm complexity and high speed. Fig.5 shows the fog/haze removal results by guided image filtering along with self-adaptive weight coefficients. The original haze image and haze removal result are illustrated in Fig. 5a and b respectively, and the coefficient τ in Fig. 5b is set to 4.2746. The original fog image and fog removal result are shown in Fig. 5d and c respectively, and τ is set to 6.0884 in Fig. 5d. As can be seen, the proposed algorithm not only retains the advantages of simplicity, validity, and no color distortion in the existing algorithms of vision enhancement, but also overcomes the shortcoming of excessive or inadequate enhancement caused by ignoring the difference of various images.

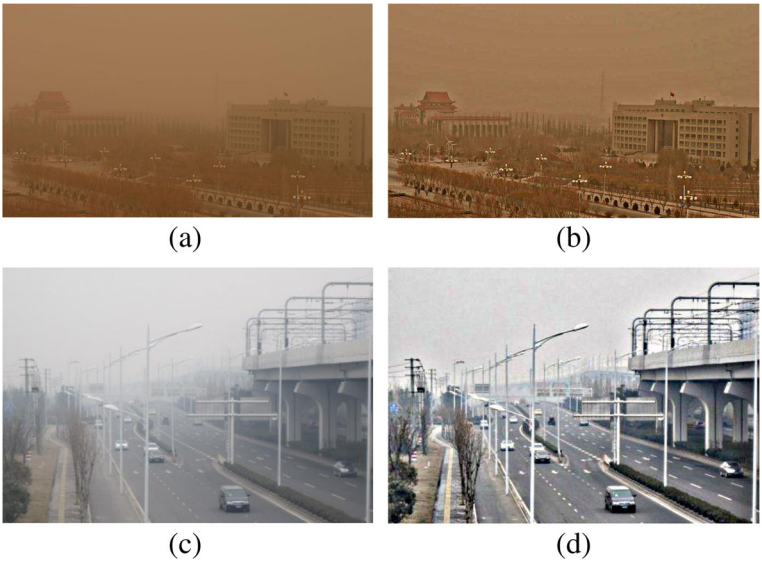

Fig. 5 Image fog/haze removal based on self-adaptive guided image filtering: (**a**) Original haze image, (**b**)Haze removal result, (**c**) Original fog image, (**d**) Fog removal result

3.3 Color correction for haze image

According to the previous recovery results, the proposed algorithm based on self-adaptive guided image filtering shows satisfactory visual effect. However, under haze weather conditions, the intensity of atmospheric scattering has a strong dependence on visible-light wavelength, which inevitably leads to phenomenon of color distortion. In Section 3.2 the image recovery is carried out in terms of improving the visibility, and the main reason for color distortion in the haze image is not taken into account. Because the sky region contains main optical information after complex scattering by the haze layer, the point of atmospheric light is the most representative position with main information of color distortion, which can be adequately employed to correct this distortion in the haze image.

Based on the statistics of RGB channel values in the sky regions of various images, we can come to the conclusions as follows: (1) For the fog image, the ratio of R:G:B is close to 1:1:1;(2) For the haze image, the values of RGB channels meet the condition of R > G > B and the ratio of R:B is close to 2:1. If the atmospheric light value meets the conclusion (1) or (2), the original degradation image can be classified as the fog image or haze image, and then the haze image will be processed by the additional step of color correction.

The atmospheric light value of haze image is firstly calculated by the dark channel operation [3], and through the RGB values of each pixel subtracting RGB values of atmospheric light in a certain proportion respectively, the color correction can be achieved eventually. The image after color distortion correction can be expressed by:

$$\begin{cases} I_c^R = I_e^R - \delta A^R \\ I_c^G = I_e^G - \delta A^G \\ I_c^B = I_e^B - \delta A^B \end{cases} \tag{6}$$

where I_e^R, I_e^G and I_e^B are the R, G, B channel values of the image after filtering enhancement respectively. A^R, A^G and A^B are the R, G, B channel values of atmospheric light point A respectively. δ is the above-mentioned correction proportion coefficient.

This operation can further improve the effect of haze removal and is advantageous for human eyes to recognize scene object. However, this color correction may weaken the intensity of haze removal image and leads to light energy attenuation. Therefore, an appropriate brightness compensation to the corrected image is performed. Fig. 6a shows the original haze image, and the haze removal images before and after color correction are illustrated in Fig. 6b and c respectively. As can be clearly seen, the color correction plays an indispensable role in image haze removal.

4 Experimental results

This section mainly focuses on the comparison between the classical algorithms of Tarel [10], Fattal [1], and He [3] and our algorithm for thick fog and haze removal. In order to best demonstrate the power of proposed algorithm, the major coefficients in the algorithms of Tarel, Fattal and He are set to the appropriate values. Moreover, the guided image filtering [4] is applied to the algorithm of He [3] to further improve the estimate accuracy of transmission map. Difficulty from this, the guided image filter is used to achieve the image fog/haze removal directly in the proposed algorithm. The experiment is performed using the software Matlab 2013b, which is installed on a computer with an Intel Core i7-4790 processor. Note that the test images in this paper are mainly taken from the Internet.

The experiments are composed of two parts, i.e., thick fog removal and haze removal experiments. The test image with thick fog is selected as the test image primarily as shown in Fig. 7a. Fig. 7b, c and d show the recovery results by the algorithms of Tarel, Fattal, He respectively, and the result by our algorithm is illustrated in Fig. 7e. In Fig. 7e the value of self-adaptive weight coefficient is calculated as 5.7621 when the N value is 7 for this fog image. Note that it is the fog image, so the color correction isn't required here. By comparison, the proposed algorithm for thick fog removal is superior to the algorithms of Tarel, Fattal and He.

In order to verify the effectiveness of proposed algorithm for recovering the haze image, an image with thick haze is selected as the test image as shown in Fig. 8a. Fig. 8b, c and d show the recovery results by the algorithms of Tarel, Fattal, and He respectively. As can be seen, the recovery results by these classical algorithms are quite limited for this haze image, and the color distortion of long-wavelength visible-light becomes more apparent in their results. Fig. 8e illustrates the result by our algorithm with self-adaptive guided image filtering. One can see that the visual effect of Fig. 8e is obviously much more outstanding than those of

Fig. 6 Color correction for haze image: (**a**) Original haze image, (**b**) Haze removal image without color correction, (**c**) Haze removal image with color correction

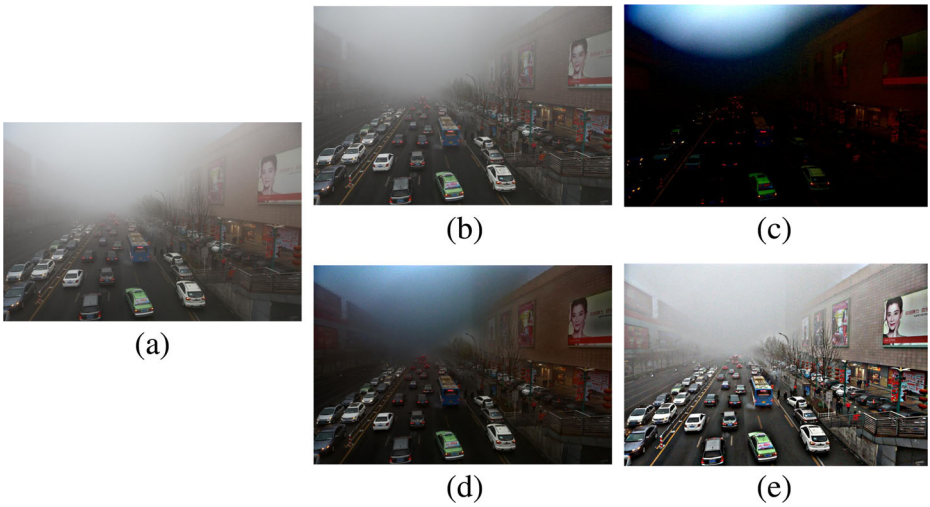

Fig. 7 Experiment on image fog removal: (**a**) Original thick fog image, (**b**) Result by Tarel, (**c**) Result by Fattal, (**d**) Result by He, (**e**) Our result

Fig. 8b, c and d. Moreover, the ultimate recovery image (see Fig. 8f) shows the high recognition of scenes after color correction using color channel information of sky region in haze image Fig. 8a. In Fig. 8e and f the value of self-adaptive weight coefficient is calculated as 3.6788 when the N value is 4 for this haze image. The value of correction proportion coefficient δ is set to 0.4 as illustated in Fig. 8f.

To further verify the advantages of our algorithm for image haze removal, another test image with different scenes is selected for experiment, and the recovery results are shown in Fig. 9. Fig. 9a shows the original haze image, Fig. 9b, c and d show the recovery results by the algorithms of Tarel, Fattal, and He respectively. The experimental result by our algorithm with self-adaptive guided image filtering is illustrated in Fig. 9e, and the ultimate recovery image

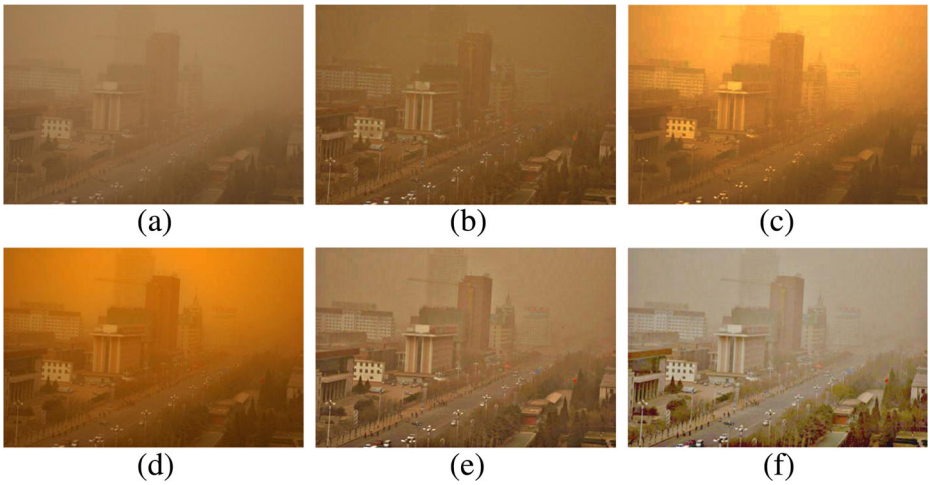

Fig. 8 Experiment I on image haze removal, (**a**) Original haze image, (**b**) Result by Tarel, (**c**) Result by Fattal, (**d**)Result by He, (**e**) Our result without color correction, (**f**) Our result with color correction

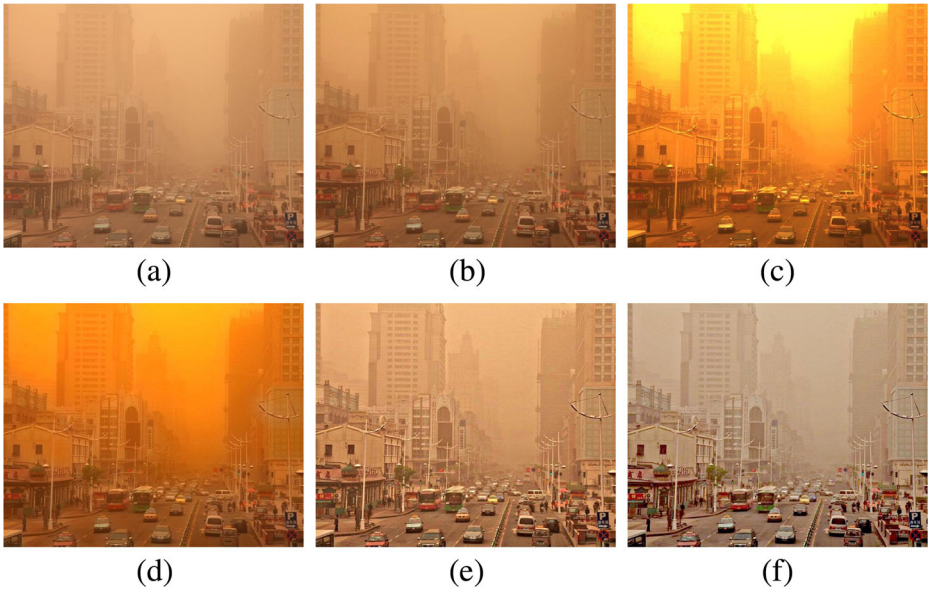

Fig. 9 Experiment II on image haze removal, (**a**) Original haze image, (**b**) Result by Tarel, (**c**) Result by Fattal, (**d**) Result by He, (**e**) Our result without color correction, (**f**) Our result with color correction

after color correction (see Fig. 9f) has more outstanding effect. By comparison, we can easily see that the proposed algorithm for haze image removal is superior to the other classical algorithm in terms of recovery effect and color correction. In Fig. 9e and f the value of self-adaptive weight coefficient is calculated as 3.1360 when the N value is 4 for this haze image. The value of correction proportion coefficient δ is set to 0.3 as illustated in Fig. 9f.

However, the recovery result by our proposed algorithm also suffers from certain shortcomings. The recovery result may appear reddish in the local region if there are some objects

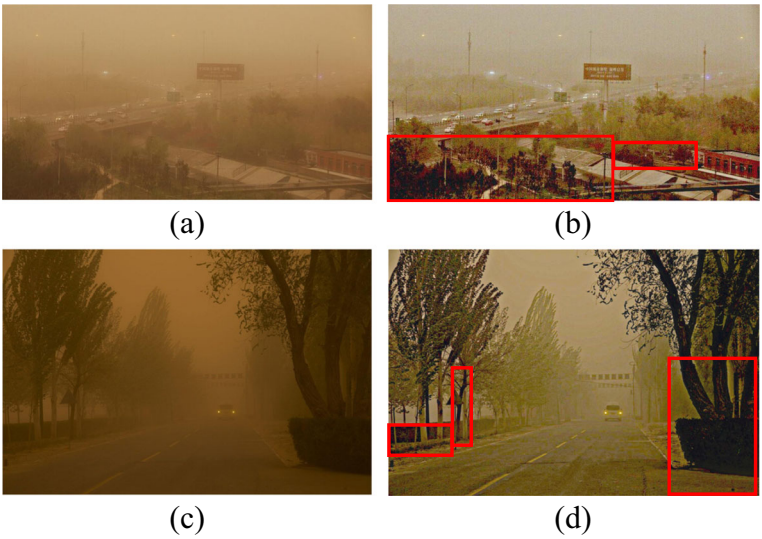

Fig. 10 Color distortion: (**a**) and (**c**) Original haze images, (**b**) and (**d**) The results of proposed algorithm

Table 1 Objective evaluation scores by no-reference quality evaluator [9]

Scene	Tarel	Fattal	He	Ours without color correction	Ours with color correction
Figure 7	19.5916	27.6512	20.1286	18.5357	/
Figure 8	27.2087	26.4108	23.6248	21.4127	20.7043
Figure 9	27.6396	27.0031	25.4323	16.0795	17.3955

whose value of one color channel is much higher than the others, e.g., the dark green trees in the recovery images as illustrated in Fig. 10b and d (indicated by the red rectangles), whose original images are shown in Fig. 10a and c respectively. In Fig. 10b the value of self-adaptive weight coefficient is calculated as 3.5460 when the N value is 4 for this haze image. The value of correction proportion coefficient δ is 0.4 here. In Fig. 10d the value of self-adaptive weight coefficient is calculated as 3.4790 when the N value is 4 for this haze image. The value of correction proportion coefficient δ is 0.35 here.

Besides the subjective evaluation above, an objective evaluation is carried out using the no-reference quality evaluator [9] in spatial domain, which can measure the loss degree of image details. A lower score indicates a better image quality. The scores of recovery results by the algorithms of Tarel, Fattal, He and ours are shown in Table 1 respectively. To be fair, all the test images are converted into JPG format here. Furthermore, two other objective evaluations, i.e., the information entropy and average gradient, are added to Section 4, which are shown in Table 2 and Table 3, respectively. As can be seen from these scores in Table 1, Table 2 and Table 3, the proposed algorithm is approximately the best ones. From the objective point of view, it is also proved that our method is effective to haze image removal.

5 Conclusion

In conclusion, we propose a simple and efficient algorithm for image fog/haze removal. With the employment of sky segmentation method and L_0 smoothing filtering, the main boundaries extraction of non-sky region is successfully realized, which facilitates

Table 2 Objective evaluation scores by the information entropy

Scene	Tarel	Fattal	He	Ours without color correction	Ours with color correction
Figure 7	11.8975	9.4886	13.0554	14.7161	/
Figure 8	10.5764	11.7948	12.1392	11.9732	12.6413
Figure 9	11.6776	13.3136	13.6929	13.2376	12.9924

Table 3 Objective evaluation scores by the average gradient

Scene	Tarel	Fattal	He	Ours without color correction	Ours with color correction
Figure 7	2.9755	1.3793	2.9657	8.0830	/
Figure 8	2.2148	1.9074	1.7432	3.3720	4.3659
Figure 9	2.4159	2.9816	2.7753	5.6983	6.0624

determining the self-adaptive weight coefficient in guided image filtering according to the images with different characteristics, and avoids the phenomenon of excessive or inadequate enhancement. For the haze image, the proposed algorithm further corrects the color distortion via the color channel information in the sky region, and thus realizes the clear and realistic recovery of haze image eventually. Experimental results on a variety of test images demonstrate the effectiveness of proposed algorithm from both the subjective and objective evaluations. In addition, not only can the proposed algorithm remove fog/haze but it can be used to classify the fog or haze image. However, it should be addressed that the proposed algorithm has some limitations.

The above-mentioned classification isn't completely automatic and also needs the RGB channel values of atmospheric light A and their proportion relationship to realize the classificatio manually. Furthermore, if the original image has large difference in its RGB channel values, the color distortion may emerge in the recovery result, and we leave this problem for future research.

Acknowledgements This work was supported by National Natural Science Foundation of China (No. 41601353, 61503300), and Foundation of Key Laboratory of Space Active Opto-Electronics Technology of Chinese Academy of Sciences (No. AOE-2016-A02), and Scientific Research Program Funded by Shaanxi Provincial Education Department (No. 16JK1765), and Natural Science Basic Research Plan in Shaanxi Province of China (No. 2014JQ8327 and 2017JQ4003) and Foundation of State Key Laboratory of Transient Optics and Photonics, Chinese Academy of Sciences (No. SKLST201614).

References

1. Fattal R (2008) Single image dehazing. ACM Trans Graph 27(3):1–9
2. Fu Z, Yang Y, Shu C, Li Y, Wu H, Xu J (2015) Improved single image dehazing using dark channel prior. J Syst Eng Electron 26(5):1070–1079
3. He K, Sun J, Tang X (2011) Single image haze removal using dark channel prior. IEEE Trans Pattern Anal Mach Intell 33(12):2341–2353
4. He K, Sun J, Tang X (2013) Guided image filtering. IEEE Trans Pattern Anal Mach Intell 35(6):1397–1409
5. Jiang B, Zhang W, Ma X, Ru Y, Meng H, Wang L (2015) Method for sky region segmentation. IET Electron Lett 51(25):2104–2106
6. Jiang B, Zhang W, Meng H, Ru Y, Zhang Y, Ma X (2015) Single image haze removal on complex imaging background. IEEE Int Conf Softw Eng Serv Sci:280–283
7. Khan SH, Bennamoun M, Sohel F, Togneri R (2016) Automatic shadow detection and removal from a single image. IEEE Trans Pattern Anal Mach Intell 38(3):431–446
8. Li B, Wang S, Zheng L (2015) Single image haze removal using content-adaptive dark channel and post enhancement. IET Comput Vis 8(2):131–140
9. Mittal A, Moorthy AK, Bovik AC (2012) No-Reference Image Quality Assessment in the Spatial Domain. IEEE Trans Image Process 21(12):4695–4708
10. Tarel JP, Hautière N (2009) Fast visibility restoration from a single color or gray level image. IEEE International Conference on computer vision: 2201–2208
11. J. Wang, N. He, L. Zhang, and K. Lu (2015) Single image dehazing with a physical model and dark channel prior. Neurocomputing 149(PB): 718–728
12. Xu L, Lu C, Xu Y, Jia J (2011) Image smoothing via L_0 gradient minimization. ACM Trans Graph 30(6):1–11
13. Yu J, Tao D, Wang M (2012) Adaptive hypergraph learning and its application in image classification. IEEE Trans Image Process 21(7):3262–3272
14. Yu T, Riaz I, Piao J, Shin H (2015) Real-time single image dehazing using block-to-pixel interpolation and adaptive dark channel prior. IET Image Process 9(9):725–734
15. J. Zhao, M. Gong, J. Liu, and L. Jiao (2014) Deep learning to classify difference image for image change detection. International Joint Conference on Neural Networks: 411–417
16. Zhu Q, Mai J, Shao L (2015) A fast single image haze removal algorithm using color attenuation prior. IEEE Trans Image Process 24(11):3522–3533